ELSEVIER

Journal of Alloys and Compounds 235 (1996) 225–231

Journal of ALLOYS AND COMPOUNDS

Electrochemical properties of the $Zr(V_{0.4}Ni_{0.6})_{2.4}$ hydrogen storage alloy electrode

X.P. Gao, W. Zhang, H.B. Yang, D.Y. Song, Y.S. Zhang, Z.X. Zhou, P.W. Shen

Institute of New Energy Material Chemistry, Nankai University, Tianjin 300071, People's Republic of China

Received 16 August 1995; in final form 16 October 1995

Abstract

In order to improve the electrocatalytic activity, hydrogen adsorption performance and activation behaviour of the $Zr(V_{0.4}Ni_{0.6})_{2.4}$ alloy electrode, the alloy powder surface was modified by HF acid solution treatment. It was found that the alloy surface was transformed from a Zr-rich layer to a Ni-rich layer after the treatment and the electrocatalytic activity, hydrogen adsorption performance and activation behaviour of the alloy electrodes were significantly improved. An electrode reaction mechanism on the alloy surface (i.e. the mechanism of nickel-catalysis, hydrogen adsorption and hydrogen-transference) has been suggested. The Ni sites on the surface are not only the electrocatalytic reaction centre but also the hydrogen adsorption centre. In addition, the impedance spectra were fitted to an equivalent circuit using a non-linear, least squares fitting program.

Keywords: Laves phase alloy; Hydride electrode; Electrocatalytic activity; Hydrogen adsorption

1. Introduction

Laves phase alloy hydrides have some promising properties as electrode materials in reversible metal hydride batteries because they have inherent advantages of high electrochemical capacity and long-term durability during electrochemical cycling. However, it is known that they have the disadvantage of requiring many charge–discharge cycles for activation. In addition, the electrocatalytic activity and hydrogen adsorption performance on the surface of the Laves phase alloy electrode was inferior to that of the $MmNi_5$-based alloy electrode. Therefore, an improvement in the electrocatalytic activity and activation behaviour of the Laves phase alloy electrode was required for electrochemical application. The activation behaviour could be changed to some extent by an oxidation treatment under low pressure oxygen [1], an anodic oxidation treatment of the particle surface [2] and an addition of small amounts of misch metal to Laves phase alloys [3]. However, the electrocatalytic activity and hydrogen adsorption performance of the electrode surface were still poor. Suda [4] had studied the $LaNi_{4.7}Al_{0.3}$ alloy by F-solution treatment, which is referred to as the 'fluorinated hydriding alloy', and found that the kinetic property of hydrogen absorption was markedly improved. This treatment method can be expanded to other classes of the hydrogen storage material as well. Züttel et al. [5] confirmed that the activation of the $Zr(V_{0.25}Ni_{0.75})_2$ alloy electrode was remarkably improved after HF treatment.

In this work, in order to solve this problem, the HF acid solution treatment was performed in $Zr(V_{0.4}Ni_{0.6})_{2.4}$ alloy. After the treatment, the electrocatalytic activity, hydrogen adsorption performance and activation behaviour of the alloy electrode were considerably improved. The electrocatalytic activity was generally characterized by electrochemical reaction resistance [6]. The hydrogen adsorption performance of the alloy surface was measured by means of cyclic voltammetry. The chemical state and composition of the alloy powder surface were analysed using X-ray photoelectron spectroscopy (XPS).

2. Experimental details

The $Zr(V_{0.4}Ni_{0.6})_{2.4}$ alloy was prepared by arc melting in an argon atmosphere. The alloy was crushed and ground mechanically to 300 mesh particle size

SSDI 0925-8388(95)02127-2

without annealing. The alloy and its hydride were then analysed by X-ray powder diffraction. The crystallographic parameters of the alloy and its hydride were calculated. The hydrogen storage performance of the alloy was measured by the desorption pressure–composition (P–C) isotherm at 30°C.The alloy powder was treated by HF acid solution (pH = 1.5–2.0) for 15 min and rinsed with distilled water and then dried in an argon atmosphere. The surface chemical state and composition of the untreated and treated alloy powders were measured by means of XPS in a PHI-5300 ESCA spectrometer using Mg Kα radiation of energy 1253.6 eV. The surface morphologies of the untreated and treated alloy powder were analysed by scanning electron microscopy (SEM).

For the electrochemical measurements, approximately 0.50 g of the alloy powder was mixed with carbonyl nickel powder (0.15 g) and polyvinyl alcohol solution and then compacted into a porous nickel substrate (2.0×2.0 cm^2) attached to the nickel rod. After that, the substrate was dried and then pressed.

The electrochemical measurements of these negative electrodes were performed using a sintered nickel electrode with a large capacity as counter electrode and a Hg|HgO|5 M KOH electrode as reference electrode. The discharge capacity was measured under a current density of 50 mA g^{-1} at ambient temperature and the cut-off potential for each discharge was set to be − 0.740 V. After activation, the electrochemical impedance spectra were carried out using a Solartron 1250 frequency response analyser in combination with a TD3690 potentiostat under the remote control of an HP Vectra 286 computer at the steady state condition. The impedance spectra of the electrodes were recorded from 10 kHz to 10 mHz and at 5 mV of the amplitude of perturbation for different depth of discharge (DOD). The impedance spectra were fitted to an equivalent circuit using a non-linear, least squares (NLLS) fitting program EQUIVCRT [7].

The cyclic voltammetry experiments were taken using a TD3690 potentiostat, controlled by an external computer. A three-electrode system with a Hg|HgO|5 M KOH reference electrode and a platinum wire counter electrode was used. The working electrodes were constructed from approximately apparent surface 1.0×1.0 cm^2 plates of alloy powders without carbonyl nickel powder.

3. Results and discussion

3.1. Structures and P–C isotherms

The structures of $Zr(V_{0.4}Ni_{0.6})_{2.4}$ alloy and its hydride were checked using X-ray diffraction (Fig. 1). It was found the alloy mainly has a cubic C15-type Laves phase structure. The residual phases were a hexagonal C14-type Laves phase and a Zr_9Ni_{11} phase. After hydrogenation, a shift of the peak to lower angles was observed, indicating that a volume expansion had occurred as a consequence of hydrogenation. The obtained lattice parameter a increased from 7.081 to 7.467 Å, indicating that the expansion $\Delta V/V$ of the alloy lattice volume was 17.2% for [H]/[M] = 0.90 at 0.1 MPa. However, the crystal structure did not change. The P–C desorption isotherm of the $Zr(V_{0.4}Ni_{0.6})_{2.4}$ alloy at 30°C is illustrated in Fig. 2. Evidently, the isotherm was sloped and had no pressure plateau region indicating formation of hydrogen in solid solution. Moreover, the residual hydrogen in the alloy at equilibrium pressure of 10^{-4} MPa was still greater. These results are in agreement with previous

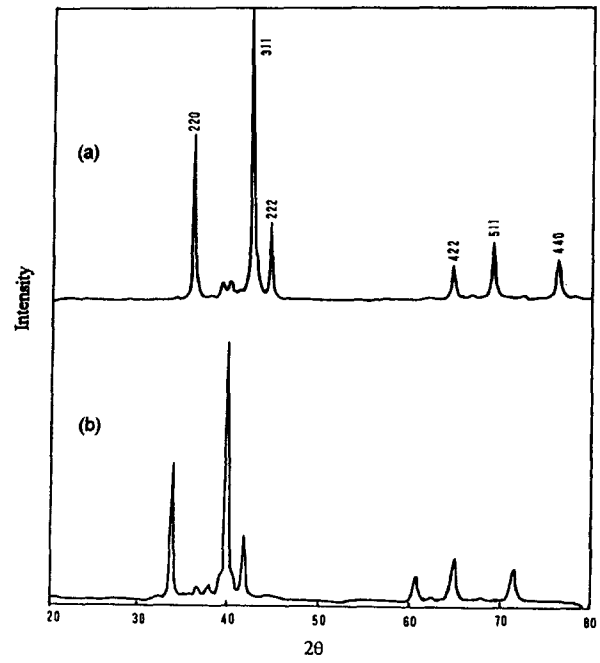

Fig. 1. X-ray diffraction patterns for (a) $Zr(V_{0.4}Ni_{0.6})_{2.4}$ alloy and (b) its hydride.

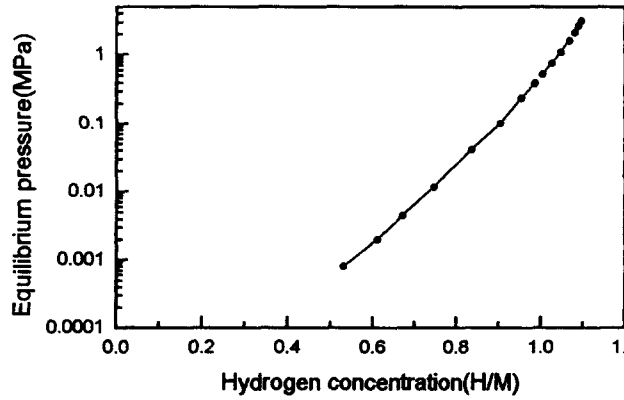

Fig. 2. P–C desorption isotherm for $Zr(V_{0.4}Ni_{0.6})_{2.4}$ alloy at 30°C.

reports on the hydrogen storage performance of the ZrV_2 alloy [8].

3.2. Surface state

Previous work has demonstrated that the as-fabricated surface of the Zr-based Laves alloy is not suitable for electrochemical charging without any treatment because of poor charge acceptance [9]. In particular, the compact thin passive ZrO_2 layer with a monoclinic structure prevents water dissociation and hydrogen penetration into the bulk [1]. In order to further investigate the effect of the HF acid solution treatment on the electrochemical properties of the alloy electrode, the surface states of the untreated and treated alloy powders were analysed by SEM and XPS techniques.

SEM micrographs for the untreated and treated $Zr(V_{0.4}Ni_{0.6})_{2.4}$ alloy powders are shown in Fig. 3. The surface of the untreated alloy powder was smooth, but the treated one was rough and cracked as a result of corrosion of oxides or metals by the HF acid solution and volume expansion of alloy grains due to hydrogen penetration into the bulk. Within pores and cracks, new clean surface was created. The BET surface area of alloy showed that the specific surface area increased from 0.10 $m^2\ g^{-1}$ in the untreated state to 0.26 $m^2\ g^{-1}$ after the treatment.

The chemical states of Zr, V and Ni were examined by determining their binding energies. The XPS analysis revealed that the zirconium and vanadium on the alloy surface were fully oxidized to ZrO_2 (181.8 eV) and V_2O_5 (516.8 eV); the nickel was partially oxidized and existed as NiO (855.7 eV) and in the metallic state (852.8 eV). After the treatment, the chemical states of the constituent elements on the alloy surface were the same as that of the untreated alloy, except for nickel, which was partially oxidized due to exposure to air in the experiment. In addition, the composition of the alloy surface changed significantly after the treatment by XPS (see Fig. 4). In general, surface segregation is a common feature in most of the alloys. The surface energy is an important factor for normal segregation. There was stronger segregation of zirconium on the untreated alloy powder surface on account of the smaller surface energy of zirconium compared with vanadium and nickel [10]. However, examination of the constituent elements on the treated alloy powder surface indicated that nickel was enriched and zirconium content had decreased. The reason is that ZrO_2 on the surface and metallic zirconium in the subsurface are more easily dissolved in HF acid solution to further form stable complex ions [11]. This treatment procedure makes the alloy surface elements selectively dissolve into the HF acid solution to form a Ni-rich alloy surface, as found in the work of Züttel et al., which can provide a strong hydrogen adsorption ability and an excellent electrocatalytic activity.

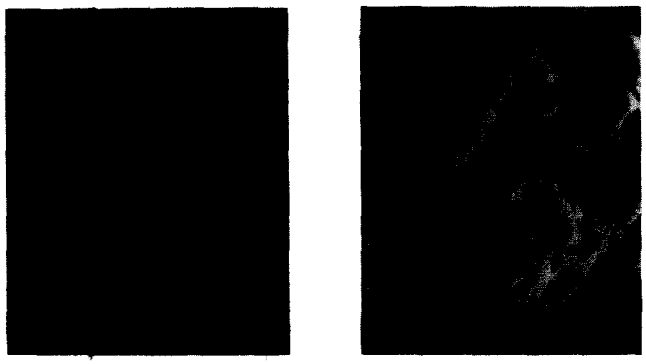

Fig. 3. SEM micrographs at 6000× for the (a) untreated and (b) treated $Zr(V_{0.4}Ni_{0.6})_{2.4}$ alloy powders.

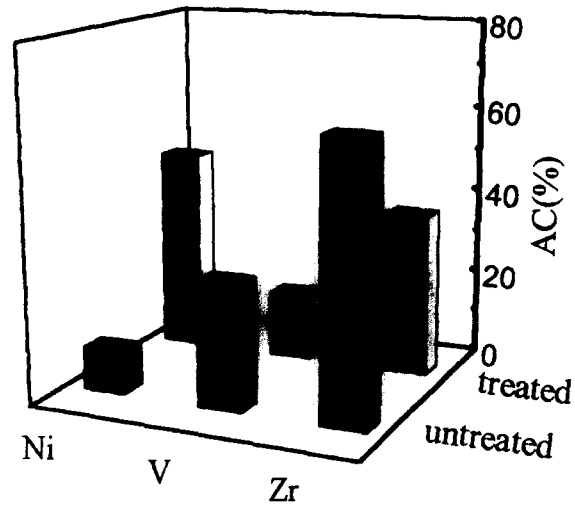

Fig. 4. The top surface atomic concentration for the untreated and treated $Zr(V_{0.4}Ni_{0.6})_{2.4}$ alloy powders by XPS.

3.3. Activation

Fig. 5 presents the variation in discharge capacity with cycle number for the $Zr(V_{0.4}Ni_{0.6})_{2.4}$ alloy electrodes untreated and treated by HF acid solution at room temperature. It was found that the untreated alloy electrode was hardly activated and that there was almost no capacity before ten cycles. However, the treated alloy electrode showed an initial capacity of approximately 80 mA h g^{-1} and a higher discharge capacity of about 230 mA h g^{-1} after ten cycles. Therefore, the treated alloy electrode exhibited an easy activation property owing to the formation of a Ni-rich surface and increased specific surface area, as pointed out above.

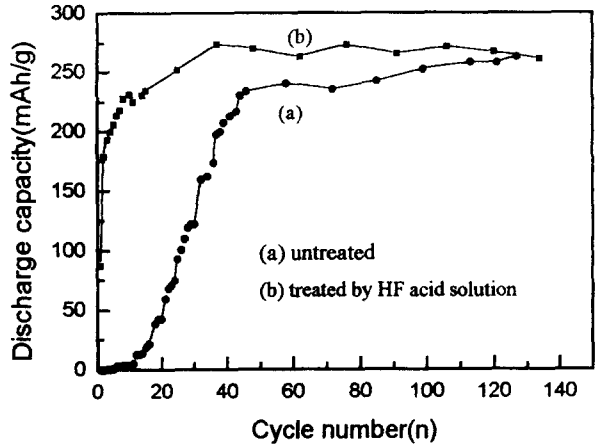

Fig. 5. Variation in discharge capacity with cycle number for the (a) untreated and (b) treated $Zr(V_{0.4}Ni_{0.6})_{2.4}$ alloy electrodes at room temperature.

After activation, the ratio of the discharge capacity at a high discharge current (250 mA g^{-1}) to the discharge capacity at a low discharge current (50 mA g^{-1}), which is referred to as the high rate dischargeability, was only about 30% for both electrodes as a result of the sloping plateau pressure in the isotherm. In contrast, the potential decreases progressively during discharging under a current density of 50 mA g^{-1} without the discharge plateau region. This is also attributed to the sloping plateau pressure.

3.4. Impedance

Electrochemical impedance spectroscopy has become a powerful tool for investigating the properties of various electrochemical systems [12], especially for the non-destructive analysis of the hydride electrode. The impedance spectra of the untreated and treated $Zr(V_{0.4}Ni_{0.6})_{2.4}$ alloy electrodes from 10 kHz to 10 mHz for different DOD are shown in Fig.6 (the numbers in the plots indicate frequency). The Cole–Cole plots mainly consisted of two obvious comparable semicircles and no slope related to the Warburg impedance. The smaller, high frequency region semicircle hardly changed, but the low frequency region semicircle changed markedly with DOD. The reaction resistances from the semicircle in the low frequency region were calculated by the fitting program. The dimension of the resistance is watt grams owing to the dimension of current which is milliamps per gram. The DOD dependence of the reaction resistance for the untreated and treated alloy electrodes is illustrated in Fig. 7. This result indicated that the reaction resistances increased with increasing DOD or decreasing hydrogen concentration in the alloy for both electrodes, as found for Ti-based alloy electrodes [6]; this is probably due to a decrease in

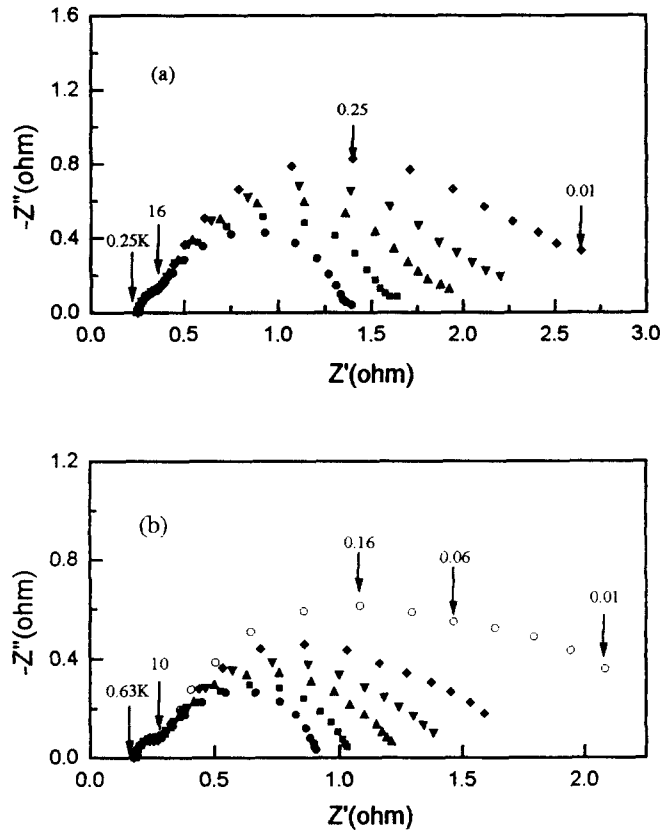

Fig. 6. Cole–Cole plots for the (a) untreated and (b) treated $Zr(V_{0.4}Ni_{0.6})_{2.4}$ alloy electrodes at different DOD: (a) DOD(%) ●, 0; ■, 25.4; ▲, 50.9; ▼, 76.3; ♦, 100; (b) DOD(%) ●, 0; ■, 20.6; ▲, 41.4; ▼, 62.1; ♦, 80.8; ○, 100.

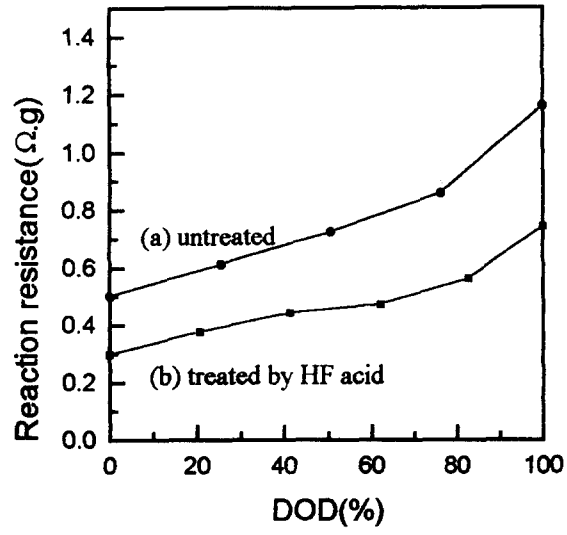

Fig. 7. DOD dependences of the reaction resistances for the (a) untreated and (b) treated $Zr(V_{0.4}Ni_{0.6})_{2.4}$ alloy electrodes.

the Fermi level with decreasing hydrogen concentration in alloy [13]. In particular, the reaction resistances of the treated alloy electrode have obviously decreased compared with those of the untreated one at the same DOD, so that the electrocatalytic activity

of the treated alloy electrode was markedly improved. Therefore, it can be concluded that the HF acid solution treatment was effective in improving the electrocatalytic activity of the alloy electrode. This result demonstrated that the Ni-rich surface is of benefit to improving electrocatalytic activity and that the water electroreduction occurs at Ni sites on the surface.

For the treated alloy electrode at 100% DOD, the semicircle in the low frequency region became two semicircles. This is related to the hydrogen adsorption process on the alloy surface. Moreover, the hydrogen adsorption process has an obvious capacitive reactance-type characteristic. An NLLS fitting calculation was performed using the equivalent circuit shown in Fig. 8. The equivalent circuit for the electrode consists of the following components: the electrolyte resistance R_1, contact resistance R_2, reaction resistance R_3, adsorption resistance R_4 and constant phase element Q_i. The measured and simulated impedance spectra over the whole frequency region are shown in Fig. 9. The fitting error was less than 3% over the measured frequency range.

Yayama et al. [14] studied the mechanism of the hydrogen evolution reaction of the $TiMn_{1.5}$ electrode in constant current electrolysis in alkaline solution and

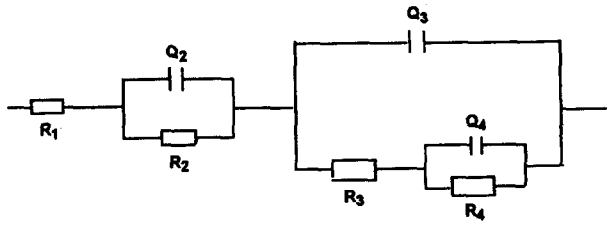

Fig. 8. An equivalent circuit of hydrogen storage electrode. $Q_i(\omega) = \{Y_{0i}(j\omega)^n\}^{-1}$ $(0 < n < 1)$.

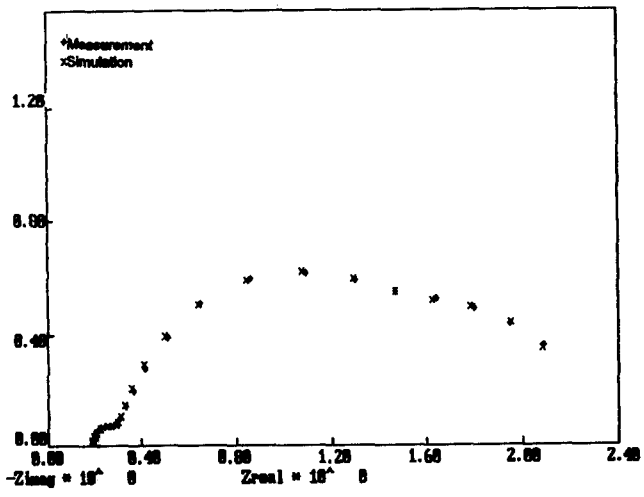

Fig. 9. The measured and simulated impedance spectra for the treated alloy electrode at 100% DOD.

found that the bulk diffusion of hydrogen in the electrode was the rate determining step. It can be seen from Cole–Cole plots of the untreated and treated alloy electrodes that there is no slope related to the Warburg impedance in the low frequency region for all discharge states. It is concluded that the bulk diffusion of hydrogen in the alloy is fast by comparison, and that the surface electrocatalytic reaction is the rate determining step except for the treated alloy electrode at 100% DOD under the steady state condition. In the later case, the rate determining step is a mixed process of the surface charge transfer and the surface hydrogen adsorption.

3.5. Cyclic voltammetry

As described in the impedance experiment of the treated alloy electrode, there was a hydrogen adsorption phenomenon. In order to further demonstrate the hydrogen adsorption mechanism on the alloy surface, cyclic voltammetry was performed. Cyclic voltammograms (CVs) of the untreated and treated alloy electrodes, obtained at variable scan rates after activation with constant current charge–discharge, are shown in Figs. 10(a) and 10(b) respectively. At a low scan rate of 1 mV s^{-1}, hydrogen was absorbed in the cathodic direction and then oxidized in the anodic direction for both electrodes. There was no hydrogen adsorption peak because of the relatively fast hydrogen diffusion in the alloy surface. At higher scan rates, a strong hydrogen-adsorption peak in the cathodic direction appeared on the alloy surface after HF treatment, in contrast to the untreated surface which was weak in hydrogen adsorption [15]. Horiuti and Polanyi [16] showed that the activation energy barrier of the electrochemical reaction process should be reduced by adsorption of the product (H_{ads}). Consequently, the hydrogen adsorption is of benefit in improving the electrocatalytic activity in agreement with the above impedance experiments. In the anodic direction, no corresponding desorption peak was observed and the electrochemical oxidation was the main reaction process at this stage of the experiment. The hydrogen adsorption peak potential shifted in the negative direction with increasing scan rate, compared with the hydrogen electrochemical oxidation peak. This indicated that hydrogen diffusion in the bulk is also a rate determining step during the transient steady state process.

In accordance with cyclic voltammetry and impedance experiments, it is considered that the hydrogen adsorption is related to the Ni-rich surface. The CVs of the carbonyl nickel electrode, presented in Fig. 10(c), also contain a similar hydrogen adsorption peak. In light of the position of the hydrogen adsorption peak in the carbonyl nickel electrode, it is reasonable to

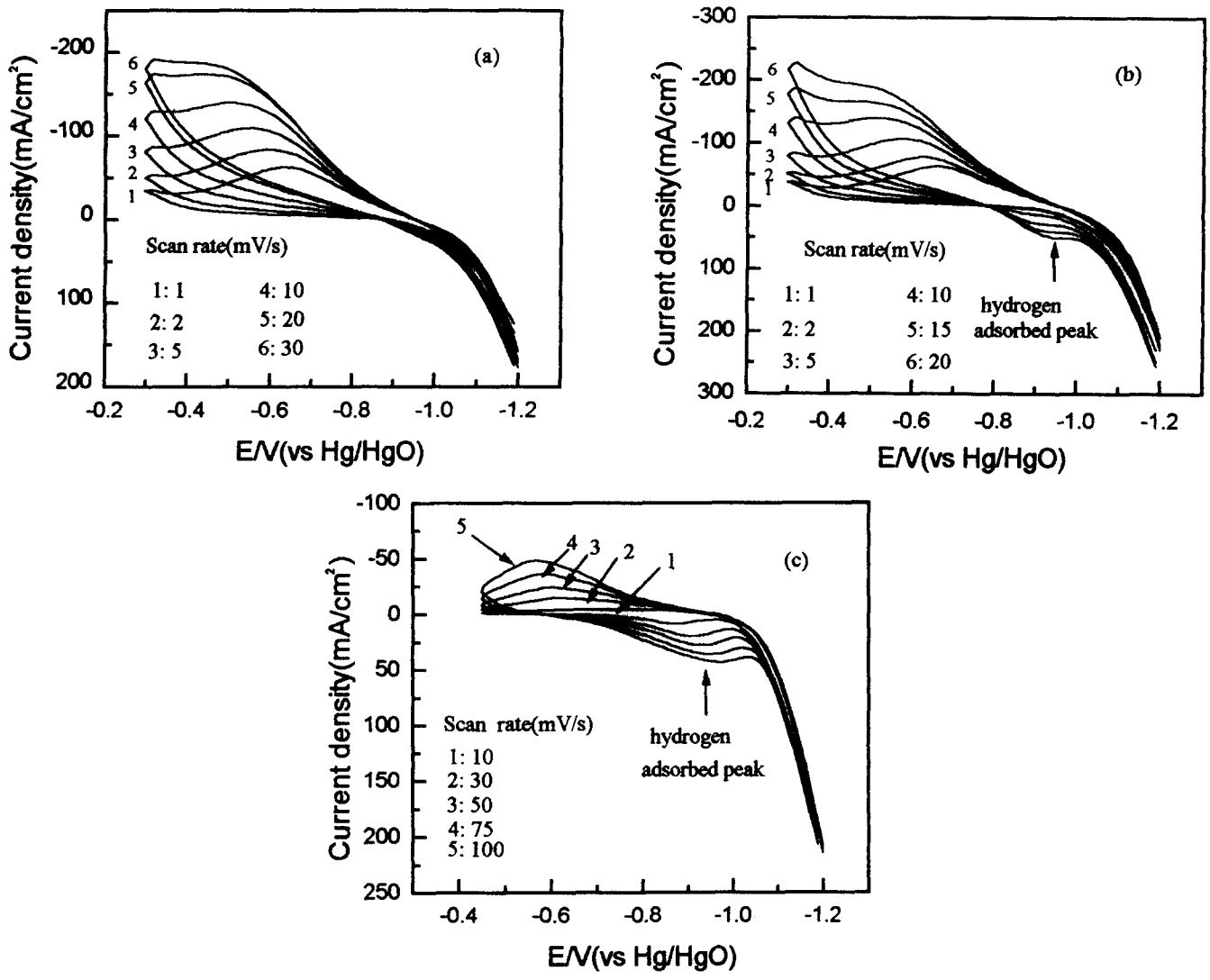

Fig. 10. CVs for: (a) untreated $Zr(V_{0.4}Ni_{0.6})_{2.4}$ alloy electrode; (b) $Zr(V_{0.4}Ni_{0.6})_{2.4}$ alloy electrode treated by HF acid solution; (c) carbonyl nickel electrode.

conclude that the hydrogen adsorption occurs at Ni sites. The steps listed below were inferred in the hydrogen storage alloy electrode reaction process:

$$Ni + H_2O + e^- \leftrightarrow NiH_{ads} + OH^- \quad (1)$$

$$NiH_{ads} + M \leftrightarrow Ni + MH_{abs} \quad (2)$$

$$MH_{abs} \overset{\text{diffusion}}{\leftrightarrow} (MH_x)_{\text{hydride}} \quad (3)$$

$$NiH_{ads} + H_2O + e^- \leftrightarrow H_2 + Ni + OH^- \quad (4)$$

$$2NiH_{ads} \leftrightarrow 2Ni + H_2 \quad (5)$$

Here, the subscripts 'ads' and 'abs' mean adsorbed and absorbed respectively; M denotes a hydrogen storage alloy. As a result of the electroreduction reaction of water, atomic hydrogen is chemically adsorbed on the surface Ni sites (reaction (1)). From the adsorbed state, hydrogen on the surface Ni sites can pass on into the absorbed state in the subsurface (reaction (2)). From this absorbed state, hydrogen can further diffuse into the bulk to form hydride (reaction (3)). However, under high cathodic overpotential (overcharged), the adsorbed hydrogen on the surface Ni sites can be decomposed, either by electrochemical desorption (reaction (4)) or by recombination (reaction (5)). It is evident that the surface Ni sites are not only the electrocatalytic reaction centre but also the hydrogen adsorption centre.

4. Conclusions

The untreated $Zr(V_{0.4}Ni_{0.6})_{2.4}$ alloy electrode is disappointing in electrocatalytic activity, hydrogen adsorption and activation behaviour. By HF acid solution treatment, the electrochemical performances of the alloy electrode were dramatically improved. This treatment procedure resulted in changes in the

surface state of the alloy powder, such as increased specific surface area and a change to a Ni-rich from a Zr-rich surface layer. These factors are of benefit to accelerating activation and improving surface electrocatalytic activity and hydrogen adsorption of the alloy electrode. During the steady state process, the rate determining step is the surface electrocatalytic reaction, except for the treated alloy electrode at 100% DOD which is a mixed process of surface charge transfer and surface hydrogen adsorption. In addition, the special impedance spectrum was fitted to an equivalent circuit using an NLLS fitting program. During the transient steady state process, the hydrogen diffusion in the bulk is the rate determining step. The Ni sites on the surface are not only the electrocatalytic reaction centre but also the hydrogen adsorption centre.

Acknowledgement

This work was supported by the National Advanced Material Committee of China (NAMCC).

References

[1] H. Sawa, M. Ohta, H. Nakano and S. Wakao, *Z. Phys. Chem. N. F., 164* (1989) 1527.
[2] S. Wakao, H. Sawa and J. Furukawa, *J. Less-Common Met., 172–174* (1991) 1219.
[3] S.R. Kim and J.Y. Lee, *J. Alloys Comp., 185* (1992) L1.
[4] S. Suda, *Nikkei Mater. Technol., 142* (1994) 71.
[5] A. Züttel, F. Meli and L. Schlapbach, *J. Alloys Comp., 209* (1994) 99.
[6] N. Kuriyama, T. Sakai, H. Miyamura I. Uehara and H. Ishikawa, *J. Alloys Comp., 202* (1993) 183.
[7] B.A. Boukamp, *Solid State Ionics, 20* (1986) 31.
[8] A. Pebler and E.A. Gulbransen, *Trans. TMS–AIME, 239* (1967) 1593.
[9] M.A. Fetcenko, S. Venkatesan, K.C. Hong and B. Reichman, *Power Sources, 12* (1989) 411.
[10] A.R. Miedema, *Z. Metallkd., 69* (1978) 287.
[11] F.A. Cotton and G. Wilkinson, *Advanced Inorganic Chemistry*, Wiley, 1972, 3rd edn., p. 822.
[12] P. Agarwal, M.E. Orazem and L.H. Garcia-Rubio, *J. Electrochem. Soc., 139* (1992) 1917.
[13] C.D. Gelatt, Jr., H. Ehrenreich and J.A. Weiss, *Phys. Rev. B, 17* (1978) 1940.
[14] H. Yayama, K. Kuroki, K. Hirakawa and A. Tomokiyo, *Jpn. J. Appl. Phys., 23* (12) (1984) 1616.
[15] R.H. Wopschll and I. Shain, *Anal. Chem., 39* (1967) 1514.
[16] J. Horiuti and M. Polanyi, *Acta Physicochim. URSS, 2* (1935) 505.